Am J Physiol Lung Cell Mol Physiol 293: L639–L650, 2007.
First published May 25, 2007; doi:10.1152/ajplung.00403.2006.

A tissue-engineered model of fetal distal lung tissue

M. J. Mondrinos,[1] S. Koutzaki,[2] P. I. Lelkes,[1] and C. M. Finck[2,3,4]

[1]*Laboratory of Cellular Tissue Engineering, School of Biomedical Engineering, Science and Health Systems, Drexel University, Philadelphia;* [2]*Department of Pediatrics and Pediatric Surgery, St. Christopher's Pediatric Associates, St. Christopher's Hospital for Children, Philadelphia;* [3]*Department of Surgery, Drexel University College of Medicine, Philadelphia; and* [4]*Department of Pediatric Surgery, Connecticut Children's Hospital, Hartford, Connecticut*

Submitted 10 October 2006; accepted in final form 7 May 2007

Mondrinos MJ, Koutzaki S, Lelkes PI, Finck CM. A tissue-engineered model of fetal distal lung tissue. *Am J Physiol Lung Cell Mol Physiol* 293: L639–L650, 2007. First published May 25, 2007; doi:10.1152/ajplung.00403.2006.—In extending our previous studies toward development of an engineered distal lung tissue construct (M. J. Mondrinos, S. Koutzaki, E. Jiwanmall, M. Li, J. P. Dechadarevian, P. I. Lelkes, and C. M. Finck. *Tissue Eng* 12: 717–728, 2006), we studied the effects of exogenous fibroblast growth factors FGF10, FGF7, and FGF2 on mixed populations of *embryonic day 17.5* murine fetal pulmonary cells cultured in three-dimensional collagen gels. The morphogenic effects of the FGFs alone and in various combinations were assessed by whole mount immunohistochemistry and confocal microscopy. FGF10/7 significantly increased epithelial budding and proliferation; however, only FGF10 alone induced widespread budding. FGF7 alone induced dilation of epithelial structures but not widespread budding. FGF2 alone had a similar dilation, but not budding, effect in epithelial structures, and, in addition, significantly enhanced endothelial tubular morphogenesis and network formation, as well as mesenchymal proliferation. The combination of FGF10/7/2 induced robust budding of epithelial structures and the formation of uniform endothelial networks in parallel. These data suggest that appropriate combinations of exogenous FGFs chosen to target specific FGF receptor isoforms will allow for control of lung epithelial and mesenchymal cell behavior in the context of an engineered system. We propose that tissue-engineered fetal distal lung constructs could provide a potential source of tissue or cells for lung augmentation in pediatric pulmonary pathologies, such as pulmonary hypoplasia and bronchopulmonary dysplasia. In addition, engineered systems will provide alternative in vitro venues for the study of lung developmental biology and pathobiology.

alveoli; distal vascular development; organotypic 3-D culture; fibroblast growth factors; collagen gel

THE PATHOLOGY OF PULMONARY hypoplasia, frequently encountered in premature birth or secondary to conditions such as congenital diaphragmatic hernia, includes reduced lung mass, insufficient surfactant production because of poorly differentiated alveolar epithelium, and reduction of alveolar gas exchange (54). Bronchopulmonary dysplasia, a pediatric lung disease that leads to respiratory distress, often occurring secondary to pulmonary hypoplasia, is hallmarked by disruption of normal late lung developmental events, culminating in reduced vascular development and alveolarization (1, 5, 11, 13). There is a great clinical need for novel strategies to augment underdeveloped or diseased lungs, which may include implantation of engineered functional pulmonary tissue or cell-based therapies. In addition to potential therapeutic applications, tissue-engineered three-dimensional (3-D) models of fetal distal lung tissue provide venues for investigating developmental interactions of lung cells in an in vitro system that is amenable to cell biological manipulations. Here we describe progress toward the development of such organotypic fetal lung tissue constructs in vitro.

Numerous studies in lung developmental biology have highlighted the importance of fibroblast growth factors (FGFs) in epithelial-mesenchymal interactions that orchestrate lung development (51). FGFs play a pleiotropic role in the development of all organs, since they affect cells derived from all three embryonic germ layers. Of the 24 or so different FGFs identified as of yet, FGFs-1, -2, -7, -9, -10, and -18 are expressed in the developing lung, and so are all the fibroblast growth factor receptors (FGFRs)-1, -2, -3, and -4 (51). In the developing lung and other organs with prominent epithelial-mesenchymal FGF signaling, epithelial cells express "b isoforms" of FGFRs, whereas mesenchymal cells express "c isoforms" (58, 59). This distinction confers FGF ligand specificity in different cell populations (42). FGF10 and FGF7 are produced in the mesenchyme and signal exclusively to epithelial cells via FGFR2b (6, 10, 24, 27, 38, 45, 49). In vitro experiments have highlighted that spatially restricted FGF10 expression in the embryonic lung mesenchyme patterns the branching/budding of the developing lung epithelium (10, 58) and potentially plays a role in lineage specification and induction of cytodifferentiation via indirect mechanisms in vivo (27). FGF7 is expressed diffusely in the subepithelial mesenchyme and induces epithelial luminal dilation via proliferation following cessation of the FGF10-induced budding (58). In contrast to the highly epithelial-specific FGF10 and FGF7, FGF2 (also known as bFGF) is more pleiotropic and binds to both the epithelial and mesenchymal isoforms of FGFRs, although higher affinity is observed for the mesenchymal c isoforms (42). FGF2 influences lung epithelial differentiation in vitro (32, 36); however, it is best known as a potent angiogenic/vasculogenic factor (8, 19, 26, 32, 46, 57). A defined role for FGF2 in lung development in vivo has yet to be established (43).

In taking a developmental biology-based tissue-engineering approach to generate an organotypic fetal lung tissue construct, we started with dissociated *embryonic day 17.5* murine fetal pulmonary cells (FPC), implementing the following three central morphological/physiological design goals: *1*) histiotypic epithelial budding and distal lung cytodifferentiation, *2*) capillary-like network assembly, and *3*) interfacing between epi-

Address for reprint requests and other correspondence: P. I. Lelkes, School of Biomedical Engineering, Science and Health Systems, Drexel Univ., Bossone 714, 3141 Chestnut St., Philadelphia, PA 19104 (e-mail: pil22@drexel.edu).

The costs of publication of this article were defrayed in part by the payment of page charges. The article must therefore be hereby marked "*advertisement*" in accordance with 18 U.S.C. Section 1734 solely to indicate this fact.

thelial and endothelial tissue components. In addition to these three basic goals, which focus on epithelial-endothelial interactions, we also sought to monitor the presence of mesenchymal cells, which influence the differentiation of epithelial and endothelial cells. As in our early work (39), we isolated FPC at *embryonic day 17.5* at the onset of the saccular (terminal airway) stage of lung organogenesis (56). Previously, we demonstrated that FPC cultured in Matrigel display enhanced epithelial growth and budding when maintained in a serum-free medium containing FGF10, FGF7, and FGF2 (39). In this permissive matrix containing a plethora of growth factors, we observed histiotypic epithelial morphogenesis when FPC were cultured in a serum-free medium devoid of growth factors or 10% FBS, albeit to a lesser degree than in the presence of the specific FGFs (39). By contrast, culturing FPC in 3-D collagen gels with either serum-free media or 10% FBS resulted in minimal epithelial morphogenesis (unpublished observations). Therefore, we tested the hypothesis that exogenous supplementation of FGF10, FGF7, and FGF2 would stimulate epithelial, and potentially endothelial, morphogenesis in 3-D collagen gel constructs.

MATERIALS AND METHODS

Fetal pulmonary cell isolation and in vitro culture. Embryonic day 17.5 (E17.5) murine FPC were obtained from the lungs of timed-pregnant Swiss Webster mouse fetuses (Charles River Laboratories), according to an approved protocol (Institutional Animal Care and Use Committee no. 30511), essentially as previously described (39). Following initial isolation, the FPC were centrifuged and resuspended in a 1.2 mg/ml liquid collagen solution (BD Biosciences) at physiological pH, at a density of 2.5–5.0 million FPC/ml. One milliliter of cell/collagen mixture per well was cast in 24-well plates and transferred to the incubator. Following polymerization of the gel, 2 ml of an 80:20 mixture of DMEM-F-12 medium (Cambrex) containing 10% FBS (Hyclone), L-glutamine, and penicillin-streptomycin antibiotics were overlaid, and the constructs were incubated overnight. Subsequently, the constructs were maintained in 2 ml serum-free basal DMEM/F-12 medium supplemented with 1% insulin-transferrin-selenium (1% ITS; BD Biosciences) and heparin (10 U/ml; Sigma); 10% FBS; or 1% ITS supplemented with FGF7 (10 ng/ml), FGF10 (25 ng/ml) or FGF2 (25 ng/ml) alone or in combination as follows: FGF10, FGF7, FGF2, FGF10/7, FGF10/7/2. All cell culture was carried out at 37°C in a 5% CO_2 humidified incubator. The medium was replaced every 48 h for the 1st wk, then every 24 h for cultures that were extended to 14 days.

Whole mount immunohistochemistry. Morphologic and phenotypic characterization of our in vitro constructs was carried out using a whole mount indirect fluorescent immunohistochemistry protocol similar to that used for whole mount staining of embryos and explants (52, 53). In brief, 3-D constructs were fixed in 4% paraformaldehyde (Electron Microscopic Sciences) for 1 h at room temperature and then overnight at 4°C and washed 3 × 20 min in 1× TBS containing 100 mM glycine (Sigma), pH = 7.4, to reduce background autofluorescence. All steps were performed at room temperature on a bench-top orbital shaker (Belly Dancer; Stovall). Constructs were washed briefly in 1× TBS and then permeabilized/blocked using 0.5% Triton X and 3% BSA in 1× TBS for 6–8 h. Following the permeabilization and blocking, constructs were washed 3 × 5 min in 1× TBS with 1% BSA. Constructs were then incubated with either polyclonal rabbit primary antibodies against pan-cytokeratin to visualize the intermediate filaments in all epithelial cells (1:100; Dako), prosurfactant protein C (pro-SP-C) to identify type II alveolar epithelial cells (AE2, 1:100; Chemicon), platelet endothelial cell adhesion molecule (PECAM)-1 (1:50; Abcam) to identify endothelial cells (ECs), and tropoelastin (1:100; Abcam) as a marker for mesenchymal cells. All primary antibodies were prepared in 1× TBS containing 0.1% Triton X and 1% BSA. Negative controls were processed identically, except that the specific primary antibodies were replaced with normal rabbit IgG (1:50 to 1:100). After washing 3 × 1 min with 1× TBS, the constructs were washed 3 × 20 min in 1× TBS with 1% BSA and then for 2 h in a large volume (15-ml tube for each sample) of 1× TBS. Samples were then washed once more with 1× TBS + 3% BSA + 0.2% Triton X for 30 min before secondary antibody application. Secondary antibodies, fluorescent goat anti-rabbit IgGs (Alexa488 or Alexa594; Invitrogen), were prepared at dilutions of 1:500 in 1× TBS containing 0.1% Triton X and 1% BSA and incubated with constructs for 2 h. Endothelial cells were identified by staining with *Griffonia simplicifolia* lectin I-isolectinB4 (isoB4; Invitrogen). Depending on the multistaining protocol, isoB4 was used conjugated to either Alexa488, Alexa568, or Alexa647. The endothelial specificity of isoB4 has been reported previously (4, 28, 30) and was also confirmed in our hands (see Fig. 3). For multiplex immunocytochemistry of vascular endothelial cell growth factor receptors (VEGFRs) and FGFRs, we used commercially available kits (Zenon anti-rabbit Alexa dye labeling kits) to generate fluorescent conjugates of rabbit polyclonal antibodies against VEGFR1 and VEGFR2 (Neomarkers) and FGFR1 and FGFR2 (Abgent) according to the manufacturer's instructions. Primary fluorescent antibody conjugates were used at 1:50 dilutions for 30 min. Staining patterns were confirmed by comparison with single-target indirect immunofluorescence in separate experiments. When double staining with isoB4 was performed, a 10 μg/ml solution of the desired isoB4 conjugate was prepared and admixed to either the secondary antibody solution or along with the primary conjugates used for multiplex immunocytochemistry. Finally, all constructs were washed 3 × 20 min with 1× TBS, then for 2 h in a large volume of 1× TBS (15-ml tube for each sample) before being mounted with antifade medium (Vectashield; Vector Laboratories), and visualization by laser-scanning confocal microscopy (Leica). Digital images were acquired using proprietary software from Leica for conventional and confocal microscopy. 3-D *z*-projections of whole mount staining were generated using the Leica confocal software.

Quantitative image analysis and statistical analysis. Quantitative analysis of phase-contrast images of alveolar-forming units (AFUs) taken at 7 days for epithelial morphometry was carried out using NIH ImageJ. Images were all taken at ×100 magnification. For each sample/condition/experiment, a minimum of 10 images containing ~25 individual AFUs were analyzed. Individual AFUs were manually outlined using the region of interest selection tool. Once selected, the area of individual AFUs (pixels) was measured. Normalized areas were calculated for each independent experiment, setting 1% ITS equal to 1. Normalized mean areas for each independent experiment were then averaged to yield a cumulative value. The data are represented as degree of increase over 1% ITS. Rudimentary bud counts for individual AFUs were performed manually in parallel with area measurements, and the results were normalized to 1% ITS in a similar fashion. Statistical analysis of the area measurements and bud counts was carried out by one-way ANOVA with the Tukey posttest (*t*-test) for individual comparisons between area values for the various media supplementation conditions.

Quantification of isoB4 staining in laser-scanning confocal micrographs was carried out using NIH ImageJ. For each experimental condition, we analyzed at least 20 randomly acquired ×200 fields at comparable *z*-positions taken from at least two whole mount constructs. Individual images were binarized, and total area of isoB4-stained pixels per ×200 microscopic field was calculated. With the same data, a morphogenetic index, termed the index of elongation and interconnectivity, was determined by measuring the fraction of total area of isoB4 staining contributed by interconnected/elongated EC area vs. single EC [index = area of interconnected EC/(area of interconnected EC + area of single EC)]. These values are basically zero for 1% ITS and 10% FBS cultures. Statistical analysis of the area

measurements was carried out by one-way ANOVA with Tukey's posttest (*t*-test) for individual comparisons between area values for the various media supplementation conditions. *P* values were calculated by Student's *t*-test with $P < 0.05$ being regarded as statistically significant.

RT-PCR. RT-PCR was used to detect steady-state mRNA expression of relevant genes in 3-D collagen gel constructs as previously reported for 3-D Matrigel (39). In brief, collagen constructs were digested, and RNA was extracted with TriReagent (Sigma) according to our previously published protocols (39). RT-PCR was performed using a commercially available kit (Promega) following the manufacturer's instructions. Primers for surfactant proteins B and C (SP-B and SP-C), FGF10, vascular endothelial growth factor A (VEGF), and glyceraldehyde-3-phosphate dehydrogenase (GAPDH), were obtained from Quiagen based on the Clontech Atlas (mouse 1.2 Array II; catalog no. 7857-1; BD Biosciences, see Table 1). For all genes, a 30-cycle PCR routine was used as previously described (39). Total RNA isolated from E17.5 fetal pulmonary tissue was used as a positive control. Negative controls included no reverse transcription samples and reactions without the addition of the cDNA template.

Viability staining. Cell viability was assessed at 7 days in select experiments by using the LiveDead kit (Invitrogen). Briefly, following removal of cell culture medium, 1 ml of 2 μM ethidium homodimer and 4 μM calcein-AM in 1× PBS were added to the constructs, which were then incubated for 30–45 min at room temperature on an orbital shaker. Samples were then washed with 1× PBS (3 × 5 min) and immediately imaged on a fluorescent microscope (Leica). Imaging was delicate, since the unfixed samples were fragile. Photobleaching of the calcein-AM during focusing in the 3-D gels was also problematic. Nevertheless, differences in the viability of cells in constructs cultured with the various media were clearly discernible.

RESULTS

Effect of FGF supplementation on epithelial morphogenesis and cytodifferentiation. We previously reported on the in vitro formation of histiotypic 3-D lung alveolar constructs in Matrigel hydrogels. Epithelial structures within these constructs, termed AFUs, were multicellular, lumen-containing assemblies that branched differentially depending on media composition (39). In expanding our prior work, we quantitatively analyzed phase-contrast micrographs of AFUs present in collagen gel constructs generated with various FGF media compositions in terms of *1*) AFU area as a measure of epithelial growth and *2*) rudimentary bud counts as a measure of epithelial morphogenesis.

Constructs cultured in basal medium supplemented with only 1% ITS (Fig. 1*A*) had the lowest levels of epithelial growth and bud formation (Fig. 1*G*); all subsequent quantitative data are normalized to this baseline condition. Of all the single FGF additions to the medium, only addition of FGF10 resulted in a statistically significant (~3-fold) increase in AFU area (Fig. 1*G*). In terms of histiotypic branching morphogenesis, the architecture of AFUs formed in FGF7 and FGF2 only conditions showed a significant yet modest increase in rudimentary bud counts (~3-fold increase over 1% ITS); however, this increase was significantly less than the approximately eightfold increase in the number of buds/AFU induced by FGF10. AFUs growing in FGF7 (Fig. 1*C*) and FGF2 (Fig. 1*D*) were dilated compared with 1% ITS and exhibited a cystic architecture without widespread bud formation. Cosupplementation of FGF10/7 did not result in statistically significant increases in AFU area or numbers of buds/AFU; however, the structures appear more dilated than in FGF10 only cultures (Fig. 1, *E* vs. *B*). FGF10/7/2 did not further enhance growth or budding of AFUs compared with FGF10/7 or FGF10 cultures (Fig. 1, *F* and *G*).

The architecture and epithelial differentiation of AFUs under various conditions were further analyzed by confocal microscopy in optical sections of whole mounts stained for cytokeratin and pro-SP-C. Negative controls were stained with normal rabbit IgG antibodies (Fig. 2*K*). In the presence of 1% ITS only, small circular structures of epithelial cells, without bud formation (Fig. 2*A*) and sparse pro-SP-C immunoreactivity (Fig. 2*B*), were observed. Culture with 10% FBS yielded the formation of slightly larger, more solid aggregates of epithelial cells with similar sparse pro-SP-C immunoreactivity (data not shown). Addition of FGF7 and FGF2 yielded largely circular AFUs with cystic morphology that displayed patchy, but consistent, pro-SP-C reactivity (Fig. 2, *C–F*). Supplementation with FGF10 alone induced a histiotypic budding architecture of the epithelial cells (Fig. 2*G*), which correlated with more uniform intense pro-SP-C staining in the cells lining these structures (Fig. 2*H*). This increased localization of pro-SP-C in AFUs was even more pronounced in cultures supplemented with either FGF10/7 (data not shown) or FGF10/7/2 (Fig. 2*J*).

In line with previous reports (14, 40), we used tropoelastin as a marker for identifying mesenchymal cells and for evaluating how exogenous FGFs might affect mesenchymal proliferation. Tropoelastin positive cells with fibroblastic morphology were present in the interstitial spaces of all constructs (Fig. 2*L*). By counting the numbers of epithelial nuclei in cytokeratin-stained AFUs and tropoelastin positive cells in the interstitial spaces, we assessed differential affects of FGF10/7 and FGF2 on epithelial and mesenchymal cell numbers in our constructs. FGF10/7 induced a statistically significant approximately fourfold increase in the number of epithelial cells per AFU (Fig. 2*M*), which correlates well with the approximately threefold increases in AFU area measured in phase-contrast

Table 1. *Primer Sequences for RT-PCR*

Gene Name	Forward Primer	Reverse Primer	Product Length (bp)
SPB	CTATCACGTCGGCCTCATCCCTG	CAGGAACTTCCGGATTGCTTCCTG	221
SPC	AGCGAGCAGACACCATCGCTACC	CTCGGAACCAGTATCATGCCCTTC	242
FGF10	AGATAACATCAGTGGAAATCGGAGTTG	GTACATTTGCCTGCCATTGTGCTGC	197
VEGF-A	CAGAAGTCCCATGAAGTGATCAAGTTC	TCACATCGGCTGTGCTGTAGGAAG	284
GAPDH	CCACTGAAGGGCATCTTGGGCTAC	CCATGAGGTCCACCACCCTGTTG	181

SPB, surfactant protein B; SPC, surfactant protein C; FGF10, fibroblast growth factor 10; VEGF-A, vascular endothelial growth factor A; GAPDH, glyceraldehyde-3-phosphate dehydrogenase.

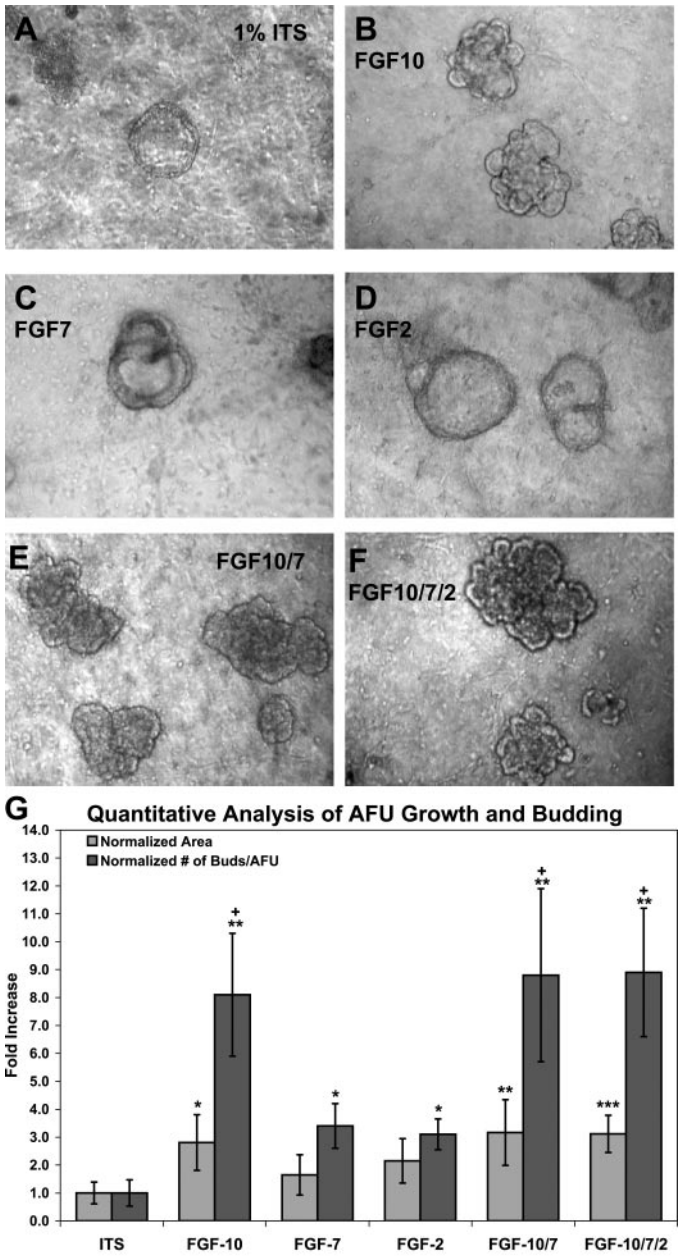

Fig. 1. Comparison of epithelial growth and morphology as a function of fibroblast growth factor (FGF) supplementation. Representative phase-contrast micrographs of alveolar-forming units (AFUs) following 7 days of culture in the presence of FGF10, FGF7, and FGF2 alone and in combination; ×100 magnification in *A–G*. *A*: 1% ITS; *B*: FGF10; *C*: FGF7; *D*: FGF2; *E*: FGF10/7; *F*: FGF10/7/2. *G*: quantification of AFU growth in response to FGF supplementation. Light gray bars: area measurements (see MATERIALS AND METHODS); data expressed as degree of increase relative to 1% ITS with statistical significance indicated vs. 1% ITS unless otherwise shown by brackets: $*P < 0.05$, $**P < 0.01$, and $***P < 0.001$. Dark gray bars: buds/AFU (see MATERIALS AND METHODS); data expressed as degree of increase relative to 1% ITS with statistical significance indicated vs. 1% ITS: $*P < 0.05$ and $**P < 0.01$. +Statistical significance indicated vs. FGF7 and FGF2 with $P < 0.05$. For both the cumulative area and bud count measurements, the no. of independent experiments was $n = 8$ for 1% ITS and FGF10/7/2 and $n = 4$ for FGF10, FGF7, FGF2, and FGF10/7 for at least 3 independent samples/experiment and a minimum of 10 microscopic fields/sample.

images (Fig. 1*G*). By contrast, FGF10/7 produced a more modest 1.5- to 2-fold increase in numbers of tropoelastin-positive cells. An approximately twofold increase in epithelial cell number per AFU (Fig. 2*M*), similar to AFU area measurements (Fig. 1*G*), was induced by FGF2. At the same time, however, FGF2 induced an ~3.5-fold increase in the numbers of tropoelastin-positive cells. FGF10/7/2 induced an approximately fourfold increase in both epithelial cells per AFU and tropoelastin-positive cell numbers (Fig. 2*M*), apparently additively combining the separately observed effects of FGF10/7 and FGF2.

Effect of FGF supplementation on endothelial morphogenesis. Based on periodic counting of isolectinB4$^+$ ECs in overnight (12–16 h) cultures of freshly isolated FPC, we know that our FPC contain ~20–30% ECs (data not shown). The endothelial phenotype of isoB4 positive cells was independently confirmed by immunofluorescence staining for VEGFR1 (Flt1) and VEGFR2 (KDR) in combination with isoB4 labeling (Fig. 3, *A–D*). In line with previous reports of VEGFR expression in fetal lung mesenchymal cells (35), VEGFR2 staining was restricted to isoB4$^+$ ECs (Fig. 3*B*), whereas VEGFR1 staining was observed both in isoB4$^+$ ECs and in most other cells of apparent mesenchymal nature (Fig. 3*C*). In 3-D gels, upon FGF supplementation, ECs formed tubular networks as visualized by PECAM-1 staining (Fig. 3*E*). In our hands, however, isoB4 staining was more uniform (Fig. 3*F*) and was therefore used for subsequent analysis, specifically for the 3-D visualization of EC tubular morphogenesis in our constructs.

3-D *z*-projections of isoB4-stained constructs revealed relatively uniform distribution of single EC within the first 24 h postseeding (Fig. 4*A*). Following 7 days of culture, all samples, with the exception of 10% FBS and 1% ITS, consistently contained elongated and interconnected ECs (Fig. 4, *B* and *C*). To quantify the degree of EC network assembly, an index of interconnectivity was calculated (see MATERIALS AND METHODS). This value is virtually zero for constructs 24 h postseeding and for constructs maintained for 7 days in 10% FBS or 1% ITS, as also confirmed visually (Fig. 4, *A–C*). The addition of any single FGF to the medium consistently yielded elongated and interconnected ECs by *day 7*. In the cases of FGF10 (Fig. 4*D*), FGF7 (Fig. 4*E*), and FGF10/7 (data not shown), a few elongated, interconnected EC networks were observed; however, there were also many single ECs. The index of interconnectivity analysis for FGF10, FGF7, and FGF10/7 yielded values ranging from ~0.2 to 0.4; however, these values were not statistically different from each other (Fig. 4*H*). Widespread, relatively uniform formation of EC networks comprising largely interconnected tubular EC assemblies was observed in the case of FGF2 (Fig. 4*F*) and FGF10/7/2 (Fig. 4*G*), as also reflected by an index of interconnectivity of ~0.8 (Fig. 4*H*). Despite the similar index of interconnectivity values for FGF2 and FGF10/7/2, the networks formed in FGF10/7/2 cultures (Fig. 4*G*) were more complex, with more and thicker branch points and consequently more connecting tubules compared with FGF2 cultures (Fig. 4*F*). Preliminary measurements of network complexity in digitally skeletonized 3-D projections of endothelial networks in FGF2 vs. FGF10/7/2 cultures indicated an approximate twofold increase in the number of branch points and the total tubule length in the presence of FGF10/7/2 compared with FGF2 alone (data not shown).

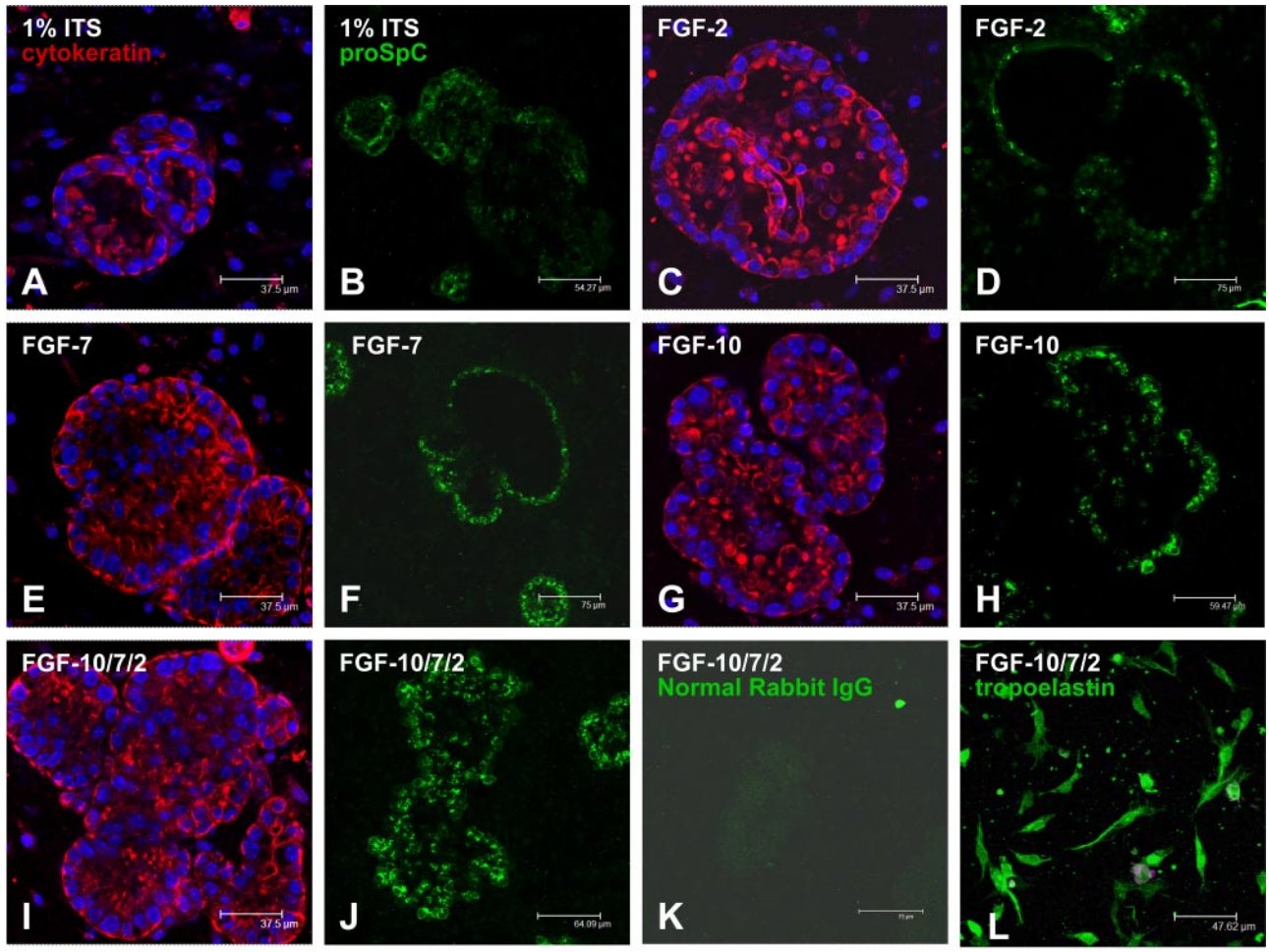

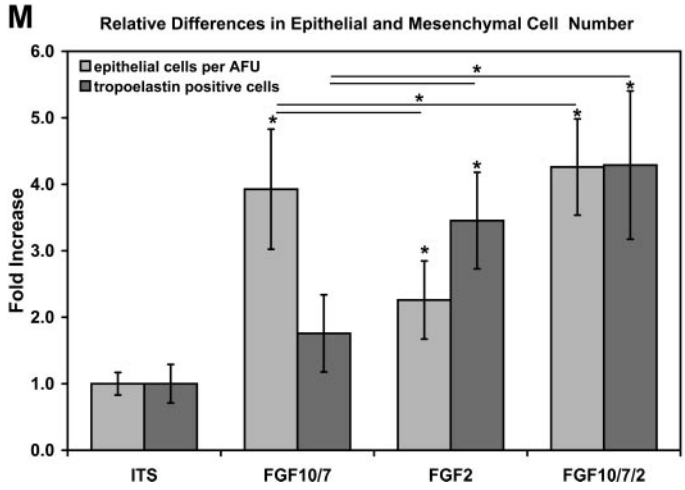

Fig. 2. Visualization of epithelial morphogenesis and cytodifferentiation. Representative optical sections through AFUs stained for cytokeratin (red) to visualize epithelial cells and counterstained with DAPI (blue) for nuclei. Nuclear staining allowed for counting of cell numbers comprising the AFUs present under the various culture conditions (*A*, *C*, *E*, *G*, and *I*) as a quantitative assessment of epithelial expansion (*M*). Cytodifferentiation was assessed by prosurfactant protein C (pro-SP-C, green) staining (*B*, *D*, *F*, *H*, and *J*). *A*: 1% ITS, scale bar = 37.5 μm. *B*: 1% ITS, scale bar = 54 μm. *C*: FGF2, scale bar = 37.5 μm. *D*: FGF2, scale bar = 75 μm. *E*: FGF7, scale bar = 37.5 μm. *F*: FGF7, scale bar = 75 μm. *G*: FGF10, scale bar = 37.5 μm. *H*: FGF10, scale bar = 50 μm. *I*: FGF10/7/2, scale bar = 37.5 μm. *J*: FGF10/7/2, scale bar = 64 μm. *K*: FGF10/7/2, normal rabbit IgG (primary antibodies are rabbit polyclonals), scale bar = 75 μm. *L*: FGF10/7/2, representative tropoelastin staining of fibroblastic cells present in the interstitial spaces used for counting, scale bar = 48 μm. *M*: quantification of epithelial cell numbers comprising AFUs, as measured by counting DAPI-stained nuclei, and mesenchymal cell numbers measured by counting tropoelastin positive cells in ×400 microscopic fields of interstitial spaces as shown in *L*. Data are expressed as degree of increase relative to 1% ITS for normalization. $*P < 0.05$ relative to baseline (1% ITS), unless otherwise shown by brackets. Data reflect comparison of at least 2 samples/condition (ITS, FGF2, FGF10/7, and FGF10/7/2 only), from $n = 3$ independent experiments, stained in parallel for both cytokeratin and tropoelastin.

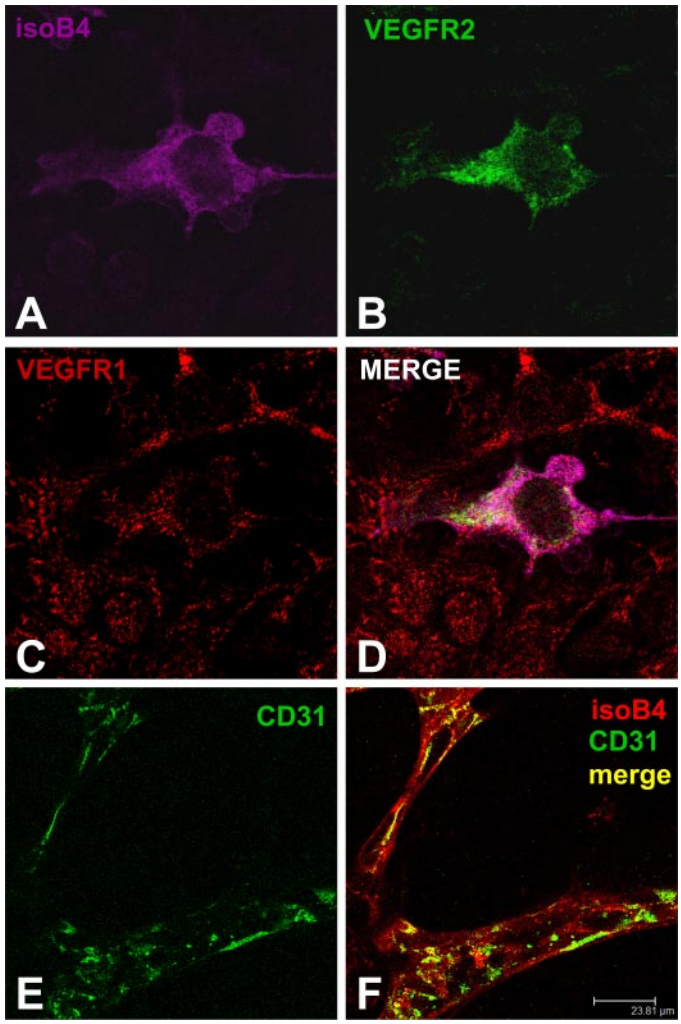

Fig. 3. Identification of endothelial cells in fetal pulmonary cell (FPC) populations. Briefly cultured FPC (overnight with 10% FBS) were triple stained for vascular endothelial growth factor receptor (VEGFR) 1 (red), VEGFR2 (green), and isolectinB4 (isoB4; magenta). IsolectinB4 positive cells (*A*, magenta) localize VEGFR2 (*B*, green) and VEGFR1 (*C*, red). Other flattened cells of apparent mesenchymal origin express VEGFR1, but not VEGFR2 (*B* and *D*). In the third dimension (3-D), endothelial cells present in FPC form tubular networks analyzed in this study. *E* and *F* show an optical section of a platelet endothelial cell adhesion molecule (PECAM)-1 whole mount stained construct, double stained with isolectinB4 and FGF10/7/2 for 7 days. *E*: PECAM-1 staining of endothelial cells in tubular networks (green) is patchy and illuminates only portions of the cell. *F*: merged image with isolectinB4 staining in the same optical plane (Alexa568 conjugate, red-orange, colocalization appears as yellow), scale bar = 24 μm.

Epithelial-endothelial interfacing with FGF supplementation. The epithelial-endothelial interface in developing AFUs was visualized by double staining for ECs (isoB4) and epithelial cells (cytokeratin or pro-SP-C). Various fluorophore combinations were used, and the marker associated with each color is clearly labeled in the panels of Figs. 1–7. Under serum-free, baseline conditions (1% ITS), most ECs remained nonelongated rounded single cells; however, some interfacing between ECs and epithelial cells was observed (Fig. 5*A*). In the case of FGF10/7/2 supplementation, AFUs were tightly interfaced with and enrobed by interconnected tubular structures comprised of ECs (Fig. 5*B*). Penetration of EC capillary-like structures in the clefts of AFUs between neighboring epithelial buds was widely observed in FGF10/7/2 cultures (Fig. 5, *B* and *C*). Pro-SP-C staining illustrates the alveolar type II epithelial nature of nearly all the cells comprising AFUs enrobed by endothelial networks in the FGF10/7/2 condition (Fig. 5*D*). Figure 5*E* shows the interfacing of pro-SP-C-expressing cells comprising bud structures and lumenized endothelial structures (Fig. 5*E*). Endothelial tubules remote from developing AFUs often appeared as "endothelial cords" that did not contain lumina; however, in areas directly contacting epithelium, consistent lumen formation was observed (Fig. 5, *E* and *F*). Shown in Fig. 5*F* are isoB4$^+$ ECs interfaced directly with an epithelial structure (inferred from the location and morphology of the DAPI-stained nuclei), which displayed continuous lumen formation (Fig. 5*F*), whereas extensions projecting in the surrounding matrix were cord-like (Fig. 5*F*).

Effect of FGF10/7/2 on construct viability and gene expression. Preliminary results suggested that growth/viability and differentiation of epithelial cells present in FPC cultured in collagen gels in basal media supplemented with either 10% FBS or 1% ITS were inferior to parallel cultures in Matrigel (unpublished observations). We hypothesized that supplementation of 1% ITS media with FGF10/7/2 would enhance epithelial viability. As seen in Fig. 6, the constructs cultured in FGF10/7/2 for 7 days contained only sparse individual dead cells and exhibited high viability in the budding epithelial structures (Fig. 6*B*). Conversely, the large spherical aggregates found in 1% ITS alone contained significant numbers of dead cells (Fig. 6*A*). Visual comparison of these images suggests that the numbers of cells in the interstitial spaces between epithelial structures is increased in FGF10/7/2 cultures, which is consistent with increased counts of tropoelastin-positive cell numbers (Fig. 2*M*). Inspection at higher magnification confirms a high degree of viability among the cells comprising the budding structures (Fig. 6*C*) and elongating tubular structures (Fig. 6*C*).

To test whether FGF10/7/2 enhanced the expression of some of the genes involved in morphogenesis and lung epithelial differentiation, we performed RT-PCR using total RNA isolated from cells cultured for 7 or 14 days. As seen in Fig. 6*D*, expression of distal epithelial marker genes SP-C and SP-B, the mesenchymal-derived morphogen FGF10, and VEGF was detected in all constructs irrespective of the media and culture time, albeit at different levels relative to GAPDH.

Expression of FGFR1 and FGFR2 in FPC input material. The action of exogenous FGFs on FPC in our constructs is presumably mediated via specific FGFRs. To confirm the presence of these receptors, we first stained FPC cultured overnight in 10% FBS for FGFR1 and FGFR2 to approximate the starting >material at the time of FGF addition. Previously, we demonstrated that these briefly cultured FPC contain islands of cytokeratin-positive epithelial cells that display tight cell-cell contact (Fig. 7*B* and Ref. 25) surrounded by a more diffuse population of flattened mesenchyme expressing vimentin filaments (Fig. 7*A*) and that a sizeable fraction of these mesenchymal cells are isoB4$^+$ ECs (39). Virtually all cells in our cultures, epithelial and mesenchymal, ubiquitously express both FGFR1 and FGFR2 protein (Fig. 7, *C–H*).

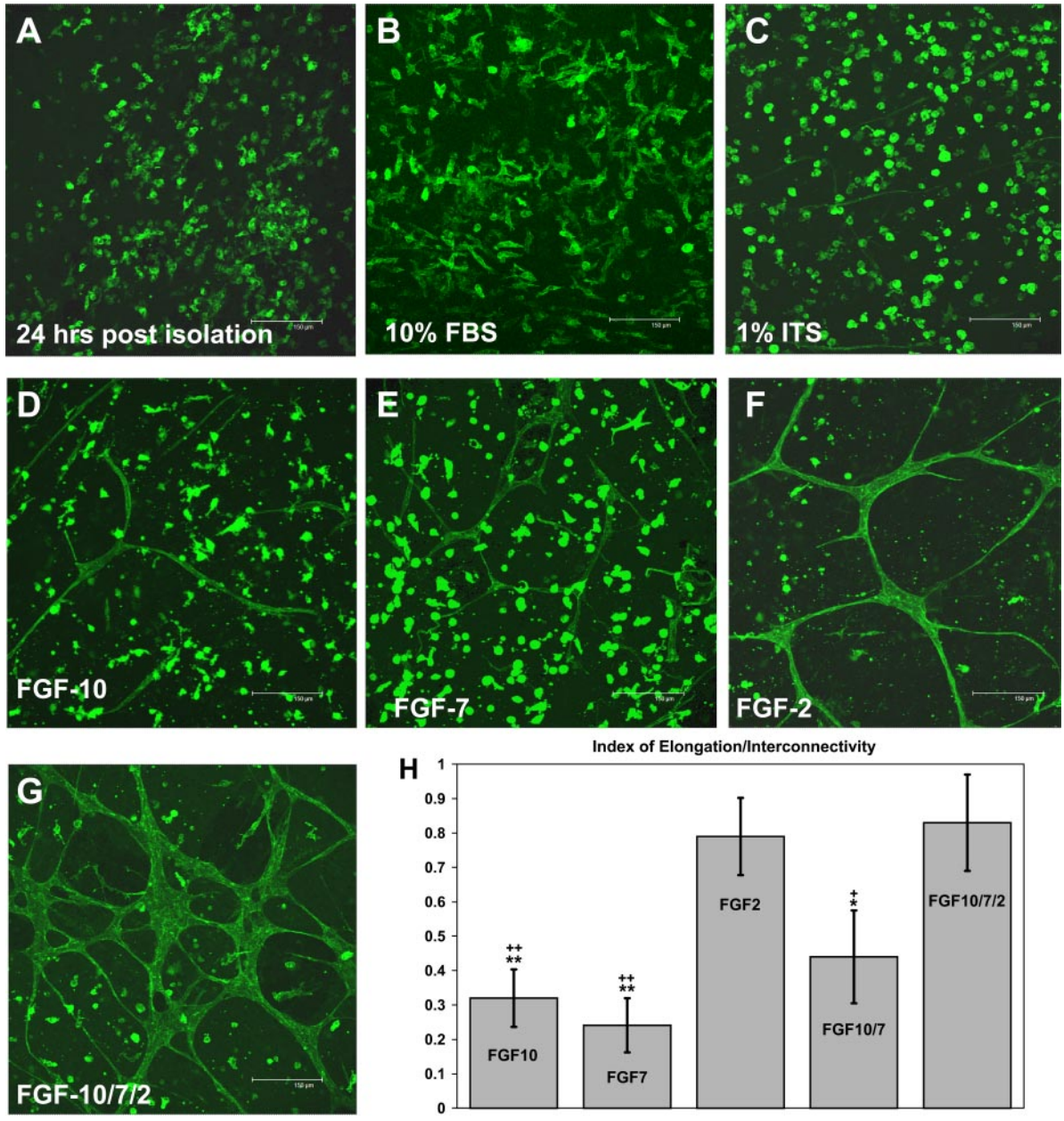

Fig. 4. FGF dependence of vascular morphogenesis following 7 days of in vitro culture, as assessed by fluorescent confocal microscopy. Images in *A–H* are 3-D *z*-projections (75- to 100-μm-thick reconstructed segments) of isolectinB4-stained constructs for endothelial cells (EC; green). *A*: distribution of endothelial cells within constructs 24 h postisolation, before application of growth factors (*day 0* of experiment). *B–G*: 7-day cultures (*B*: 10% FBS; *C*: 1% ITS; *D*: FGF10; *E*: FGF7; *F*: FGF2; *G*: FGF10/7/2). Scale bar = 150 μm in *A–G*. *H*: quantitative image analysis of isolectinB4 staining of endothelial network formation across FGF supplementation conditions. Minimum of 2 samples, 20 images/sample in $n = 8$ independent experiments for 1% ITS and 10% FBS and FGF10/7/2, and $n = 4$ independent experiments for FGF10, FGF7, FGF2, and FGF10/7. $^{**}P < 0.01$ compared with FGF10/7/2. $^{*}P < 0.05$ compared with FGF10/7/2. $++P < 0.01$ compared with FGF2. $+P < 0.05$ compared with FGF2.

DISCUSSION

Tissue engineering traditionally aims at the development of tissue constructs for therapeutic purposes, as an alternative to organ transplantation. In addition, attempts at lung tissue engineering could potentially provide the field of lung biology with high-fidelity 3-D tissue models. The establishment of organotypic fetal lung cell culture models has been reported (17, 18, 40, 44, 48); however, to the best of our knowledge, our system is the first 3-D organotypic cell culture model containing epithelial, endothelial, and mesenchymal cells, which describes effects of defined culture conditions on each of these cell types in an engineered system. Specifically, in this study, we characterized differential effects of FGF10, FGF7, and FGF2 on histiotypic distal lung morphogenesis in 3-D collagen gel constructs in vitro.

The first attempts at developing 3-D fetal lung cell culture models were reported 30 years ago by Douglas and coworkers (17, 18), focusing on organotypic culture of dispersed rodent fetal lung cells on 3-D substrates composed of gelatin/collagen. Additional early work focused on fetal and/or adult rodent

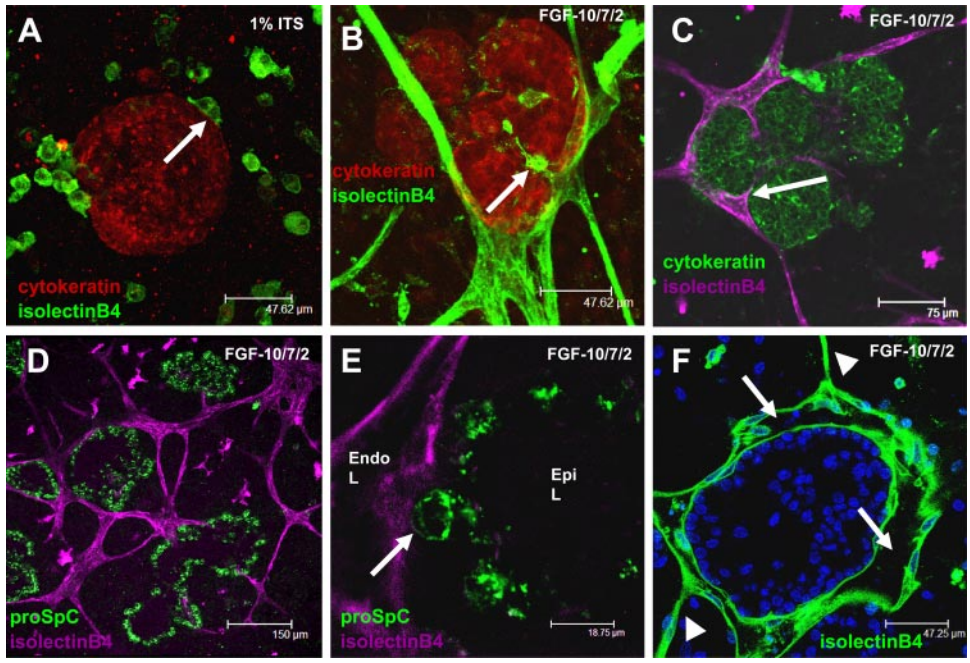

Fig. 5. Visualization of epithelial-endothelial interfacing by fluorescent confocal microscopy of whole mount-stained constructs. Representative 3-D *z*-projections (75- to 100-μm-thick reconstructed segments) of AFU structures in 7-day constructs maintained in either 1% ITS (*A*) or FGF10/7/2 (*B*) with epithelial cells cytokeratin labeled (red) and endothelial cells isolectinB4 labeled (green), scale bar = 48 μm. Note the polarized appearance of the single EC tightly interfaced with the AFU in *A* (arrow). By contrast, the AFU in *B* vs. in the FGF10/7/2-supplemented medium is enrobed by interconnected EC (arrow). *C*: penetration of developing epithelial clefts by capillary-like structures (arrow) is visualized by juxtaposition of cytokeratin (epithelial, green) and isolectinB4 (EC, magenta), scale bar = 75 μm. In FGF10/7/2 cultures, nearly all cells in the AFUs that interface with forming capillary networks are distal epithelial in nature (*D* and *E*). *D*: thin *z*-projection (20-μm-thick segment) showing pro-SP-C expression (green) of cells comprising AFUs and endothelial network formation (isolectinB4, magenta) of FGF10/7/2 over 7 days, scale bar = 150 μm. *E*: single ultrathin confocal optical section (0.1 μm) through an AFU stained with isolectinB4 (EC, magenta) and pro-SP-C (green) showing tight interfacing between endothelia-lined lumen (Endo L) and a developing distal epithelial bud forming its own lumen (indicated by Epi L) with FGF10/7/2 over 7 days, scale bar = 18 μm. *F*: single optical section of isolectinB4 (EC, green) and DAPI (nuclei, blue) staining in an AFU highlights the formation of endothelial lumina in cells contacting epithelium (arrows, note that epithelial cells are inferred by the nuclear arrangement of the cells comprising the structure in this image), as well as the thin, nonlumenized extensions in the surrounding matrix not contacting apparent epithelium (arrowheads) with FGF10/7/2 for 7 days, scale bar = 47 μm.

alveolar type II cell-enriched cultures on various matrixes, such as floating collagen membranes (21), recombined basement membrane (Matrigel; see Ref. 12), and collagen gel-based systems (55). Schuger et al. (47) used cultures of E12-E17 murine FPC to examine how addition of soluble extracellular matrix proteins affects formation of 3-D aggregates of embryonic lung cells in agitated culture on a rotary shaker. That study focused largely on the formation of the epithelial-mesenchymal interface, but not vascular development (44). Using a 3-D Gelfoam (collagen) scaffold, Nakamura et al. (40) utilized organotypic cultures of E19 rat FPC to determine the effects of dexamethasone and mechanical stretch on gene expression. More recently, in an experimental system similar to ours, Schwarz et al. (48) used organotypic mixtures of E15-E17 FPC seeded on two-dimensional (2-D) tissue culture plastic to investigate the role of ECs in epithelial-mesenchymal interactions. Our system differs significantly from that of Schwarz et al. (48) in that the cells are embedded in 3-D gels, which allows for the establishment of true 3-D cell polarity. Furthermore, at the collagen concentrations used, our system provides a mechanical environment more similar to that of soft tissues than rigid tissue culture plastic (44). The importance of compliant 3-D culture in hydrogels and the drawbacks of 2-D culture on plastic for modeling of tissues with an epithelial component have been described previously (33).

Previous studies have shown that primary AE2 cells cultured on 2-D plastic surfaces typically lose their phenotypic characteristics, such as surfactant protein expression and transition from a cuboidal to a flattened morphology reminiscent of type I alveolar epithelial cells (29, 41, 50). Some AE2 characteristics can be maintained in 2-D by plating the cells on specific extracellular matrix proteins (29, 50) and supplementing the media with various hormones and growth factors (41, 50). In addition, 2-D coculture with lung fibroblasts enhances the differentiated properties of AE2 cells as assessed by the expression of surfactant proteins (23, 34), stressing the importance of organotypic coculture of epithelial and mesenchymal cells. However, a major problem with cocultures of primary epithelial cells and fibroblasts, from lung and other sources, is fibroblast overgrowth, and many techniques have been developed to remove fibroblasts (7, 16). In our experience, the two key elements of the culture system that limit fibroblast overgrowth are the use of serum-free medium and 3-D culture. In our system, we can use specific factors, such as FGF2, to induce mesenchymal proliferation in a more controlled manner (Fig. 2*M*).

In our 3-D constructs, concerted epithelial and endothelial morphogenesis is impacted by organotypic coculture and addition of exogenous FGFs. However, our previous studies demonstrated that coculture and serum-free culture with

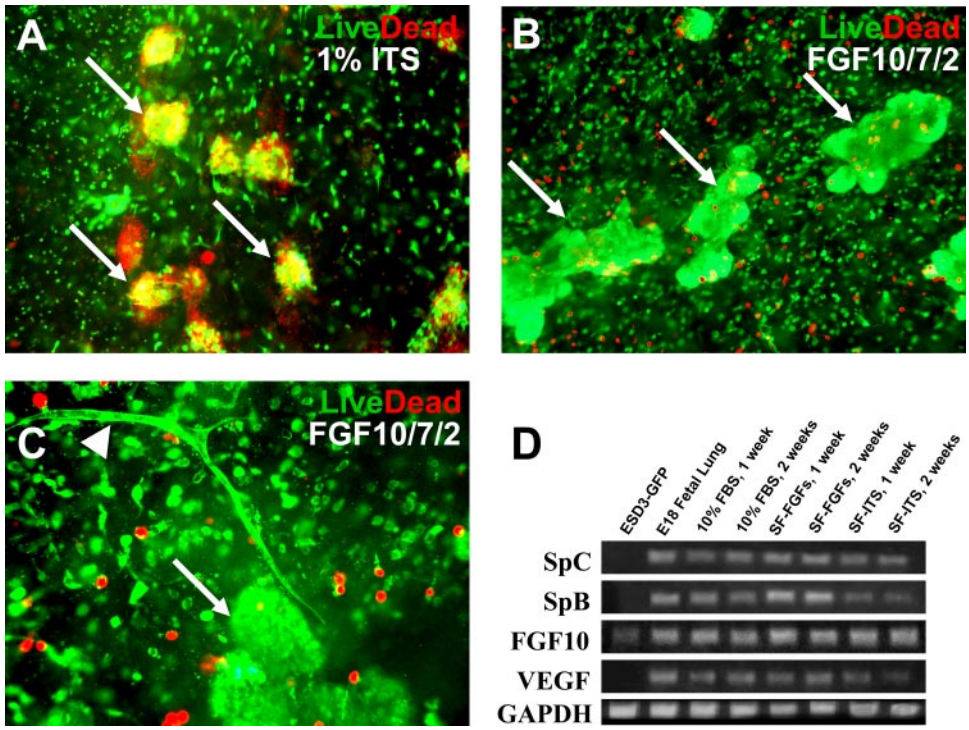

Fig. 6. Viability staining and gene expression analysis of collagen gel constructs. *A*: 1% ITS, 7 days, ×100, note the large aggregates of dead cells (red) consistent in morphology with cystic AFUs present in 1% ITS cultures demonstrated in earlier figures (arrows). *B*: FGF10/7/2, 7 days, ×100, note the presence of large budding structures comprised of nearly all viable cells (green, arrows). *C*: FGF10/7/2, 7 days, ×400, at higher magnification, note the excellent viability of the cells comprising epithelial buds (arrow) and endothelial tubules (arrowhead). Epithelial and endothelial identity in these images is inferred by morphology correlated with phenotypic staining in Figs. 2 and 5. *D*: RT-PCR analysis for lung epithelial differentiation markers SP-C and SP-B and mesenchymal-derived morphogen FGF10 and vascular endothelial growth factor-A (VEGF). Glyceraldehyde-3-phosphate dehydrogenase (GAPDH) was used as a loading control. SF-ITS = 1% ITS; SF-FGFs = FGF10/7/2.

FGF10/7/2 alone was insufficient to induce epithelial morphogenesis or maintain SP-C gene expression in extended cultures on synthetic polymer scaffolds (39). In our 3-D collagen gel constructs, endogenous signaling elaborated in serum-free culture in the absence of exogenous FGFs was insufficient to induce epithelial or endothelial morphogenesis (Fig. 5*A*). An increase in the number of dead cells in cultures maintained with 1% ITS only (Fig. 6*A*) suggests that, in the absence of serum, exogenous FGF10/7/2 function in part as survival/mitogenic factors for FPC cultured in collagen gels. Our data suggest that FGF10/7 alone induce an approximately fourfold increase in epithelial cell numbers in AFUs, whereas FGF2 alone induces a similar approximately fourfold increase in mesenchymal cell numbers, which is combined additively in FGF10/7/2 cultures (Fig. 2*M*). Taken together, the current data and our previous studies (39) suggest that FGF10/7/2 enhance viability and proliferation of FPC in 3-D culture, whereas the mechanospatial cues present in compliant hydrogels, such as Matrigel (39) and collagen gels, appear to allow for a morphogenic response. By contrast, the response of these cells to rigid polymer scaffolds is similar to 2-D culture (39). Therefore, a 3-D matrix, permissive to cell-cell and cell-growth factor interactions in an engineered system, must satisfy some basic biochemical and mechanical requirements. It is well known that growth factor signaling in vivo depends on appropriate matrix signaling and that a cross talk between these two types of signals is essential to cellular processes (2).

Both endoderm-derived lung epithelium and the lung mesenchyme express FGFR1 and FGFR2; however, epithelial cells express the b isoforms, whereas cells of mesenchymal origin express the c isoforms, and this confers ligand specificity (42, 51, 58, 59). Studies using engineered cell lines that expressed individual FGFR isoforms revealed that FGF10 and FGF7 bind only FGFR2b, whereas FGF2 binds FGFR1b, FGFR1c, and FGFR2c (42). We demonstrate here that virtually all of our FPC express FGFR1 and FGFR2 protein (Fig. 7, as a caveat, our polyclonal antibodies did not recognize/discriminate the specific isoforms). Based on the known receptor specificity of FGF10 and FGF7, we believe that exogenous FGF10 and FGF7 signal exclusively to epithelial cells through FGFR2b. Similarly, based on known binding affinities, we believe that FGF2 signals to both mesenchymal and epithelial isoforms of FGFR1 and FGFR2, with preference for mesenchymal isoforms (42). This notion is supported by the increase in mesenchymal proliferation (tropoelastin-positive cell numbers) and EC network assembly in response to FGF2, and the specific effect of FGF10/7 on epithelial proliferation (epithelial cells/AFU) and budding, which are combined upon cosupplementation with FGF10/7/2 (Figs. 2 and 4).

In line with its definitive role in inducing epithelial branching in vivo (38), FGF10 significantly enhanced bud formation in our in vitro model, an effect that was not further enhanced by cosupplementation with FGF7 and FGF2 (Figs. 1 and 2). This supports previous findings showing that exogenous FGF10 induces generalized epithelial budding in mesenchyme-free cultures in vitro and rescues alveolar growth in a nitrofen-induced model of pulmonary hypoplasia in rats (47). In our system, FGF10 is supplemented homogenously in the medium; however, there is also endogenous FGF10 gene expression by mesenchymal cells in our preparations (Fig. 6*D*). This could possibly lead to the elaboration of local gradients, although the budding response appears to be general and not patterned in any way relative to other cells in the constructs. Cosupplementation of FGF10/7 did not significantly increase measured AFU areas and budding compared with FGF10 cultures (Fig. 1*G*); however, AFUs in FGF10/7 cultures appeared more dilated (Fig. 1*E* vs. 1*B*), consistent with a proposed role for FGF7 in epithelial dilation (58). Our RT-PCR results (Fig. 6*D*) demon-

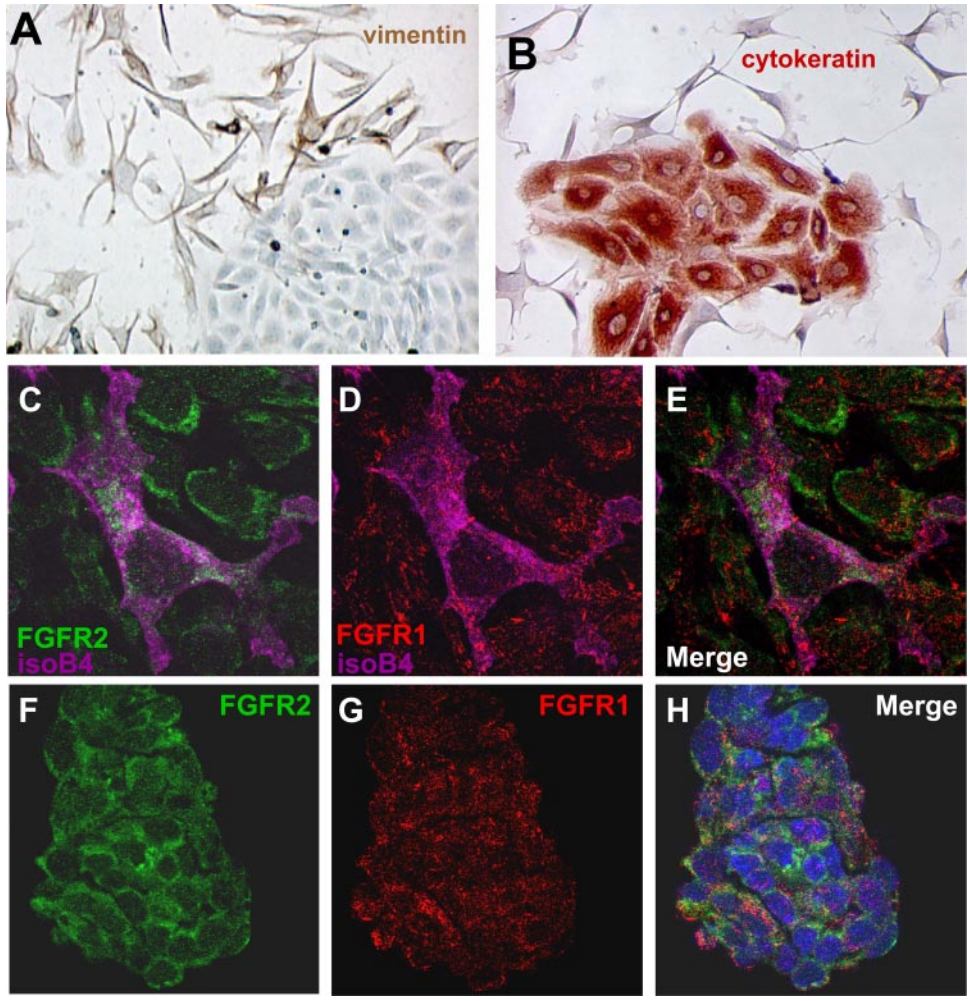

Fig. 7. Immunohistochemical detection of FGF receptors, FGFR1 and FGFR2, in briefly cultured FPC. *A*: immunoperoxidase staining for vimentin filaments in cells of mesenchymal origin (DAB, brown), ×200 magnification. *B*: immunoperoxidase staining for cytokeratin filaments (AEC, red), ×400 magnification. *C–E*: FGFR2/isolectinB4 (*C*) and FGFR1/isolectinB4 (*D*) staining of apparent mesenchymal cells and the subpopulation of endothelial cells. Virtually all other dispersed apparent mesenchymal cells express FGFR1 and FGFR2 (merged image in *E*). *F–H*: FGFR2 (*F*) and FGFR1 (*G*) staining in clustered cells of epithelial origin (inferred by morphology here) demonstrating that epithelial cells express both FGFR1 and FGFR2 (merged image with DAPI staining in *H*).

strating expression of the epithelial differentiation marker genes SP-C and SP-B across conditions suggest that baseline epithelial cytodifferentiation is retained in 3-D organotypic cultures and may be enhanced, but is not induced, by exogenous FGF supplementation. Because low levels of pro-SP-C protein expression are observed in cystic AFUs in 1% ITS cultures, we cannot conclude that exogenous FGF10/7/2 positively regulate SP-C gene expression in our system. At this stage, we suggest that the enhanced pro-SP-C immunoreactivity observed in FGF10, FGF10/7, and FGF10/7/2 cultures (Fig. 2) may reflect increased proliferation of SP-C-expressing cells present in the input material or enhanced paracrine signaling in these conditions.

Developmental interactions between lung epithelial and ECs (25) have not been studied nearly as extensively as interactions between lung epithelium and lung mesenchyme. However, tissue recombination experiments have demonstrated that lung epithelium is required for differentiation of distal lung mesenchymal progenitors in ECs, suggesting that the epithelium may orchestrate distal pulmonary vasculogenesis (20). Endothelial cells are required for development of the liver (37) and pancreas (31), even before establishment of perfused vasculature, suggesting an instructive role for the EC in organogenesis of these endoderm-derived tissues. Although such a distinct role has not yet been established in lung development, evidence illustrating the potential instructive role of vascular development in regulating lung epithelial development has been reported in both in vitro (48) and in vivo systems (60). For example, Schwarz et al. (48) reported that ablation of endothelial network formation by endothelial monocyte-activating polypeptide (EMAP) II inhibited formation of quasi-3-D cystic epithelial aggregates. Importantly, this study highlighted that EMAP II enhances the expression of fibronectin but not laminin, which may indicate that EMAP II inhibits epithelial development via alteration in the balance of extracellular matrix molecules, rather than a vascular-derived signal. Similarly, in murine embryonic lung allografts transplanted in the renal capsule, inhibition of vascular development using soluble VEGFR1 resulted in decreased vascular and saccular epithelial development (60). However, because lung epithelial cells express VEGFRs (15), this effect may also have been a direct inhibitory effect on epithelial proliferation or differentiation and does not unequivocally support the notion that discrete vascular signals regulate epithelial growth and branching. More recent experiments using sonic hedgehog-deficient embryonic lung explants demonstrated that stimulation of vascular development with exogenous angiogenic factors, angiopoietin-1 and FGF2, promoted increased epithelial branching morphogenesis (57). However, because these angiogenic factors also increased mesenchymal proliferation, it is not clear in

the study by van Tuyl et al. (57) whether increased epithelial branching was caused by enhanced mesenchymal signaling or increased vascularization.

In our system, robust epithelial-endothelial interfacing was observed in FGF10/7/2 cultures; however, we have demonstrated that the individual FGFs have differential effects on epithelial and mesenchymal cells. Addition of any single FGF resulted in significant epithelial growth (Figs. 1*G* and 2*M*) and EC elongation/interconnection; however, robust epithelial budding and uniform EC network assembly were only observed in parallel in FGF10/7/2 cultures. No significant differences in epithelial cell numbers or buds per AFU were observed when comparing FGF10/7 and FGF10/7/2 cultures (Figs. 1 and 2), despite increased vascular development (Fig. 4*G*) and mesenchymal proliferation (Fig. 2*M*) observed in FGF10/7/2 cultures. Importantly, FGF2 only cultures, in which enhanced mesenchymal proliferation (Fig. 2*M*) was accompanied by uniform endothelial network formation (Fig. 4*F*), did not display robust epithelial proliferation and budding when compared with FGF10/7 cultures (Figs. 1*G* and 2*M*). We suggest that FGF2-induced vascular development (tubular morphogenesis) in our system results from a combination of both direct effects on EC via FGFRs (Fig. 7) and indirect effects, e.g., via increased mesenchymal cell numbers (Fig. 2*M*), which in turn elaborate increased levels of angiogenic factors. It is known that pulmonary mesenchymal cell-derived VEGFs contribute to pulmonary vascular development (22). Preliminary comparison of network complexity in FGF10/7/2 vs. FGF2 cultures, which indicated an apparent twofold increase in network complexity (data not shown) despite almost no differences in mesenchymal proliferation (Fig. 2*M*), suggests that enhanced epithelial growth and budding induced by FGF10/7 positively influence vascular development. Distal epithelial cells express high levels of VEGF in vivo (3); therefore, increased epithelial cell numbers in FGF10/7/2 cultures likely result in increased levels of proangiogenic paracrine signaling. This is further supported by the observation that, in the presence of FGF10/7, which signal exclusively to epithelial cells, endothelial tubular network formation is initiated, which does not occur in baseline conditions. Therefore, we conclude that factors that promote epithelial and mesenchymal viability and proliferation, also increasing paracrine signaling activity to EC, positively impact vascular morphogenesis in this engineered system. Taken together, our data suggest that mesenchymal-derived factors, such as FGF10/7, play a more significant role in promoting epithelial proliferation and budding than a potential vascular-derived signal and that increased epithelial growth and branching positively impact vascular development.

In summary, we have developed organotypic fetal lung tissue constructs using E17.5 FPC and a combination of 3-D culture in collagen type I gels and a serum-free medium containing FGF10, FGF7 and FGF2. FGF10/7 mostly influenced epithelial budding and proliferation, whereas FGF2 alone promoted EC network assembly and induced mesenchymal proliferation. Importantly, EC network complexity increased upon cosupplementation with FGF10/7/2, suggesting positive contribution of increased epithelial budding and proliferation to vascular development. This in vitro model of fetal distal lung tissue is potentially useful for investigating lung developmental biology, in particular dynamic epithelial-endothelial interactions, and to dissect the role of mesenchymal cells in these processes. Finally, this work may also lay the groundwork for development of tissue engineering-based therapies for lung augmentation in pediatric and potentially adult pulmonary medicine.

ACKNOWLEDGMENTS

We thank Dr. Peter L. Jones (University of Pennsylvania) for helpful comments and suggestions.

GRANTS

This work was supported in part by National Institutes of Health Grant 1R21 EB-003520-01A1, grants from the St. Christopher's Foundation and the Nanotechnology Institute of Southeastern Pennsylvania, and a Drexel Synergy grant.

REFERENCES

1. **Abman SH.** Bronchopulmonary dysplasia: "a vascular hypothesis." *Am J Respir Crit Care Med* 164: 1755–1756, 2001.
2. **Acosta JM, Thebaud B, Castillo C, Mailleux A, Tefft D, Wuenschell C, Anderson KD, Bourbon J, Thiery JP, Bellusci S, Warburton D.** Novel mechanisms in murine nitrofen-induced pulmonary hypoplasia: FGF-10 rescue in culture. *Am J Physiol Lung Cell Mol Physiol* 281: L250–L257, 2001.
3. **Akeson AL, Greenberg JM, Cameron JE, Thompson FY, Brooks SK, Wiginton D, Whitsett JA.** Temporal and spatial regulation of VEGF-A controls vascular patterning in the embryonic lung. *Dev Biol* 264: 443–455, 2003.
4. **Akeson AL, Cameron JE, Le Cras TD, Whitsett JA, Greenberg JM.** Vascular endothelial growth factor-A induces prenatal neovascularization and alters bronchial development in mice. *Pediatr Res* 57: 82–88, 2005.
5. **Ambalavanan N, Carlo WA.** Bronchopulmonary dysplasia: new insights. *Clin Perinatol* 31: 613–628, 2004.
6. **Arman E, Haffner-Krausz R, Gorivodsky M, Lonai P.** Fgfr2 is required for limb outgrowth and lung-branching morphogenesis. *Proc Natl Acad Sci USA* 96: 11895–11899, 1999.
7. **Assoian RK, Schwartz MA.** Coordinate signaling by integrins and receptor tyrosine kinases in the regulation of G1 phase cell-cycle progression. *Curr Opin Genet Dev* 11: 48–53, 2001.
8. **Babaei S, Teichert-Kuliszewska K, Monge JC, Mohamed F, Bendeck MP, Stewart DJ.** Role of nitric oxide in the angiogenic response in vitro to basic fibroblast growth factor. *Circ Res* 82: 1007–1015, 1998.
9. **Bates SR, Gonzales LW, Tao JQ, Rueckert P, Ballard PL, Fisher AB.** Recovery of rat type II cell surfactant components during primary cell culture. *Am J Physiol Lung Cell Mol Physiol* 282: L267–L276, 2002.
10. **Bellusci S, Grindley J, Emoto H, Itoh N, Hogan BL.** Fibroblast growth factor 10 (FGF10) and branching morphogenesis in the embryonic mouse lung. *Development* 124: 4867–4878, 1997.
11. **Bhatt AJ, Pryhuber GS, Huyck H, Watkins RH, Metlay LA, Maniscalco WM.** Disrupted pulmonary vasculature and decreased vascular endothelial growth factor, Flt-1, and TIE-2 in human infants dying with bronchopulmonary dysplasia. *Am J Respir Crit Care Med* 164: 1971–1980, 2001.
12. **Blau H, Guzowski DE, Siddiqi ZA, Scarpelli EM, Bienkowski RS.** Fetal type 2 pneumocytes form alveolar like structure and maintain long-term differentiation on extracellular matrix. *J Cell Physiol* 136: 203–214, 1988.
13. **Bourbon J, Boucherat O, Chailley-Heu B, Delacourt C.** Control mechanisms of lung alveolar development and their disorders in bronchopulmonary dysplasia. *Pediatr Res* 57: 38R–46R, 2005.
14. **Bruce MC, Honaker CE.** Transcriptional regulation of tropoelastin expression in rat lung fibroblasts: changes with age and hyperoxia. *Am J Physiol Lung Cell Mol Physiol* 274: L940–L950, 1998.
15. **Compernolle V, Brusselmans K, Acker T, Hoet P, Tjwa M, Beck H, Plaisance S, Dor Y, Keshet E, Lupu F, Nemery B, Dewerchin M, Van Veldhoven P, Plate K, Moons L, Collen D, Carmeliet P.** Loss of HIF-2alpha and inhibition of VEGF impair fetal lung maturation, whereas treatment with VEGF prevents fatal respiratory distress in premature mice. *Nat Med* 8: 702–710, 2002 (erratum in *Nat Med* 8: 1329, 2002).
16. **Dobbs LG.** Isolation and culture of alveolar type II cells. *Am J Physiol Lung Cell Mol Physiol* 258: L134–L147, 1990.

17. **Douglas W, Moorman G, Teel R.** The formation of histotypic structures from monodisperse fetal rat lung cells cultured on a three dimensional substrate. In Vitro 12: 373–381, 1976.
18. **Douglas W, Teel R.** An organotypic in vitro model system for studying pulmonary surfactant production by type II alveolar pneumocytes. *Am Rev Respir Dis* 113: 17–23, 1976.
19. **Flamme I, Risau W.** Induction of vasculogenesis and hematopoiesis in vitro. *Development* 116: 435–439, 1992.
20. **Gebb SA, Shannon JM.** Tissue interactions mediate early events in pulmonary vasculogenesis. *Dev Dyn* 217: 159–169, 2000.
21. **Geppert EF, Williams MC, Mason RJ.** Primary culture of rat alveolar type II cells on floating collagen membranes. *Exp Cell Res* 128: 363–374, 1980.
22. **Greenberg JM, Thompson FY, Brooks SK, Shannon JM, McCormick-Shannon K, Cameron JE, Mallory BP, Akeson AL.** Mesenchymal expression of vascular endothelial growth factors D and A defines vascular patterning in developing lung. *Dev Dyn* 224: 144–153, 2002.
23. **Griffin M, Bhandari R, Hamilton G, Chan YC, Powell JT.** Alveolar type II cell-fibroblast interactions, synthesis and secretion of surfactant and type I collagen. *J Cell Sci* 105: 423–432, 1993.
24. **Guo L, Degenstein L, Fuchs E.** Keratinocyte growth factor is required for hair development but not for wound healing. *Genes Dev* 10: v165–v75, 1996.
25. **Hislop AA.** Airway and blood vessel interaction during lung development. *J Anat* 201: 325–334, 2002.
26. **Hughes GC, Biswas SS, Yin B, Coleman RE, DeGrado TR, Landolfo CK, Lowe JE, Annex BH, Landolfo KP.** Therapeutic angiogenesis in chronically ischemic porcine myocardium: comparative effects of bFGF and VEGF. *Ann Thorac Surg* 77: 812–818, 2004.
27. **Hyatt BA, Shangguan X, Shannon JM.** FGF-10 induces SP-C and Bmp4 and regulates proximal-distal patterning in embryonic tracheal epithelium. *Am J Physiol Lung Cell Mol Physiol* 287: L1116–L1126, 2004.
28. **Hyink DP, Tucker DC, St John PL, Leardkamolkarn V, Accavitti MA, Abrass CK, Abrahamson DR.** Endogenous origin of glomerular endothelial and mesangial cells in grafts of embryonic kidneys. *Am J Physiol Renal Fluid Electrolyte Physiol* 270: F886–F899, 1996.
29. **Isakson BE, Lubman RL, Seedorf GJ, Boitano S.** Modulation of pulmonary alveolar type II cell phenotype and communication by extracellular matrix and KGF. *Am J Physiol Cell Physiol* 281: C1291–C1299, 2001.
30. **Laitinen L.** Griffonia simplicifolia lectins bind specifically to endothelial cells and some epithelial cells in mouse tissues. *Histochem J* 19: 225–234, 1987.
31. **Lammert E, Cleaver O, Melton D.** Role of endothelial cells in early pancreas and liver development. *Mech Dev* 120: 59–64, 2003.
32. **Lebeche D, Malpel S, Cardoso WV.** Fibroblast growth factor interactions in the developing lung. *Mech Dev* 86: 125–136, 1999.
33. **Lee GY, Kenny PA, Lee EH, Bissell MJ.** Three-dimensional culture models of normal and malignant breast epithelial cells. *Nat Methods* 4: 359–365, 2007.
34. **Linge C, Green MR, Brooks RF.** A method for removal of fibroblasts from human tissue culture systems. *Exp Cell Res* 185: 519–528, 1989.
35. **Majka S, Fox K, McGuire B, Crossno J Jr, McGuire P, Izzo A.** Pleiotropic role of VEGF-A in regulating fetal pulmonary mesenchymal cell turnover. *Am J Physiol Lung Cell Mol Physiol* 290: L1183–L1192, 2006.
36. **Matsui R, Brody JS, Yu Q.** FGF-2 induces surfactant protein gene expression in foetal rat lung epithelial cells through a MAPK-independent pathway. *Cell Signal* 11: 221–228, 1999.
37. **Matsumoto K, Yoshitomi H, Rossant J, Zaret KS.** Liver organogenesis promoted by endothelial cells prior to vascular function. *Science* 294: 559–563, 2001.
38. **Min H, Danilenko DM, Scully SA, Bolon B, Ring BD, Tarpley JE, DeRose M, Simonet WS.** Fgf-10 is required for both limb and lung development and exhibits striking functional similarity to Drosophila branchless. *Genes Dev* 12: 3156–3161, 1998.
39. **Mondrinos MJ, Koutzaki S, Jiwanmall E, Li M, Dechadarevian JP, Lelkes PI, Finck CM.** Engineering three-dimensional pulmonary tissue constructs. *Tissue Eng* 12: 717–728, 2006.
40. **Nakamura T, Liu M, Mourgeon E, Slutsky A, Post M.** Mechanical strain and dexamethasone selectively increase surfactant protein C and tropoelastin gene expression. *Am J Physiol Lung Cell Mol Physiol* 278: L974–L980, 2000.
41. **Olsen CO, Isakson BE, Seedorf GJ, Lubman RL, Boitano S.** Extracellular matrix-driven alveolar epithelial cell differentiation in vitro. *Exp Lung Res* 31: 461–482, 2005.
42. **Ornitz DM, Xu J, Colvin JS, McEwen DG, MacArthur CA, Coulier F, Gao G, Goldfarb M.** Receptor specificity of the fibroblast growth factor family. *J Biol Chem* 271: 15292–15297, 1996.
43. **Ortega S, Ittmann M, Tsang SH, Ehrlich M, Basilico C.** Neuronal defects and delayed wound healing in mice lacking fibroblast growth factor 2. *Proc Natl Acad Sci USA* 95: 5672–5677, 1998.
44. **Paszek MJ, Zahir N, Johnson KR, Lakins JN, Rozenberg GI, Gefen A, Reinhart-King CA, Margulies SS, Dembo M, Boettiger D, Hammer DA, Weaver VM.** Tensional homeostasis and the malignant phenotype. *Cancer Cell* 8: 241–254, 2005.
45. **Post M, Souza P, Liu J, Tseu I, Wang J, Kuliszewski M, Tanswell AK.** Keratinocyte growth factor and its receptor are involved in regulating early lung branching. *Development* 22: 3107–3115, 1996.
46. **Ribatti D, Urbinati C, Nico B, Rusnati M, Roncali L, Presta M.** Endogenous basic fibroblast growth factor is implicated in the vascularization of the chick embryo chorioallantoic membrane. *Dev Biol* 170: 39–49, 1995.
47. **Schuger L, Skubitz AP, Gilbride K, Mandel R, He L.** Laminin and heparan sulfate proteoglycan mediate epithelial cell polarization in organotypic cultures of embryonic lung cells: evidence implicating involvement of the inner globular region of laminin beta 1 chain and the heparan sulfate groups of heparan sulfate proteoglycan. *Dev Biol* 179: 264–273, 1996.
48. **Schwarz MA, Wan Z, Liu J, Lee MK.** Epithelial-mesenchymal interactions are linked to neovascularization. *Am J Respir Cell Mol Biol* 30: 784–792, 2004.
49. **Sekine K, Ohuchi H, Fujiwara M, Yamasaki M, Yoshizawa T, Sato T, Yagishita N, Matsui D, Koga Y, Itoh N, Kato S.** Fgf10 is essential for limb and lung formation. *Nat Genet* 21: 138–141, 1999.
50. **Shannon JM, Pan T, Nielsen LD, Edeen KE, Mason RJ.** Lung fibroblasts improve differentiation of rat type II cells in primary culture. *Am J Respir Cell Mol Biol* 24: 235–244, 2001.
51. **Shannon JM, Hyatt BA.** Epithelial-mesenchymal interactions in the developing lung. *Annu Rev Physiol* 66: 625–645, 2004.
52. **Sillitoe RV, Hawkes R.** Whole-mount immunohistochemistry: a high-throughput screen for patterning defects in the mouse cerebellum. *J Histochem Cytochem* 50: 235–244, 2002.
53. **Snow HE, Riccio LM, Mjaatvedt CH, Hoffman S, Capehart AA.** Versican expression during skeletal/joint morphogenesis and patterning of muscle and nerve in the embryonic mouse limb. *Anat Rec A Discov Mol Cell Evol Biol* 282: 95–105, 2005.
54. **Suen HC, Catlin EA, Ryan DP, Wain JC, Donahoe PK.** Biochemical immaturity of lungs in congenital diaphragmatic hernia. *J Pediatr Surg* 28: 471–477, 1993.
55. **Sugihara H, Miyabara S, Fujiyama C, Yonemitsu N.** Reconstruction of alveolus like structure from alveolar type II epithelial cells in three dimensional collagen gel matrix culture. *Am J Pathol* 142: 783–792, 1993.
56. **Ten Have-Opbroek AA.** Lung development in the mouse embryo. *Exp Lung Res* 17: 111–130, 1991.
57. **van Tuyl M, Groenman F, Wang J, Kuliszewski M, Liu J, Tibboel D, Post M.** Angiogenic factors stimulate tubular branching morphogenesis of sonic hedgehog-deficient lungs. *Dev Biol* 303: 514–526, 2007.
58. **White AC, Xu J, Yin Y, Smith C, Schmid G, Ornitz DM.** FGF9 and SHH signaling coordinate lung growth and development through regulation of distinct mesenchymal domains. *Development* 133: 1507–1517, 2006.
59. **Zhang X, Stappenbeck TS, White AC, Lavine KJ, Gordon JI, Ornitz DM.** Reciprocal epithelial-mesenchymal FGF signaling is required for cecal development. *Development* 133: 173–180, 2006.
60. **Zhao L, Wang K, Ferrara N, Vu TH.** Vascular endothelial growth factor co-ordinates proper development of lung epithelium and vasculature. *Mech Dev* 122: 877–886, 2005.